

Tagging High Energy Photons in the H1 Detector at HERA

V.F. Andreev¹, A.S. Belousov¹, A.M. Fomenko¹, L.A. Gorbov¹, T. Greenshaw²,
E.I. Malinovski¹, S.J. Maxfield², A.V. Semenov³, I.P. Sheviakov¹, P.A. Smirnov¹,
J.V. Soloviev¹, G.-G. Winter⁴.

¹*Lebedev Physical Institute, Moscow, Russia.*

²*Department of Physics, University of Liverpool, Liverpool, UK.*

³*Institute for Theoretical and Experimental Physics, Moscow, Russia.*

⁴*DESY, Hamburg, Germany.*

Abstract

Measures taken to extend the acceptance of the H1 detector at HERA for photo-production events are described. These will enable the measurement of electrons scattered in events in the high y range $0.85 < y < 0.95$ in the 1998 and 1999 HERA run period. The improvement is achieved by the installation of an electromagnetic calorimeter, the ET8, in the HERA tunnel close to the electron beam line 8 m downstream of the H1 interaction point in the electron direction. The ET8 will allow the study of tagged γp interactions at centre-of-mass energies significantly higher than those previously attainable. The calorimeter design and expected performance are discussed, as are results obtained using a prototype placed as close as possible to the position of the ET8 during the 1996 and 1997 HERA running.

1 Introduction

The HERA accelerator at DESY brings into collision electrons (or positrons) with energy 27.5 GeV and protons with energy 820 GeV (920 GeV from 1998 onwards). A large proportion of the resulting interactions can be considered to occur between protons and essentially real photons, that is, photons for which $Q^2 \sim 0$, where $Q^2 = -q^2$ and q is the four-momentum of the photon exchanged between the electron and the proton. The energy, E_γ , of the photons in these photoproduction interactions can be related to the energies E_e and E'_e of the electron in the initial and final states through the expression

$$y = 1 - \frac{E'_e}{E_e} + \frac{Q^2}{4E_e^2} \simeq 1 - \frac{E'_e}{E_e} = \frac{E_\gamma}{E_e}.$$

Here y is the Bjorken scaling variable defined by $y = p \cdot q / p \cdot k$ and p and k are the four-vectors of the initial proton and electron, respectively. Measuring the energy of the outgoing electron enables the deduction of the photon's energy; the photon is then said to have been "tagged". Currently, photons can be tagged in the H1 detector over the y ranges $0.3 < y < 0.8$ and $0.08 < y < 0.15$, as the scattered electrons then fall within the acceptance of the existing electron taggers ET and ET44. These consist of electromagnetic calorimeters located 33.4 m and 44 m from the interaction point in the electron direction, the negative z direction in the HERA co-ordinate system.

This paper describes a calorimeter, the ET8, which has been added to the electron tagger system for the 1998 and 1999 HERA running, and the results obtained using a prototype thereof. The detector is located at $z \simeq -8$ m, enabling the detection of electrons scattered with low energy and hence the measurement of the scattered electron in photoproduction interactions in which the photon exchanged has very high energy. In addition, modifications to the beam-pipe have been made in this region, allowing the egress of the electrons through a thin window, minimising the energy loss and scattering they suffer before measurement. The ET8 covers the y range $0.85 < y < 0.95$. With the original HERA beam energies this extends the centre-of-mass energy range over which photoproduction interactions can be studied up to $W_{\gamma p} = 293$ GeV, the increased HERA proton beam energy of 920 GeV allows a centre-of-mass energy of 310 GeV to be reached. As is illustrated in figure 1, determination of the photon-proton cross-section becomes possible at an energy significantly above that of the current highest energy results[1]. In conjunction with measurements of jets in the hadronic final state, the ET8 enables the study of the partonic content of the photon in a region in which the partons carry a very small proportion of the photon's momentum[2], corresponding to the low Bjorken- x region which HERA has shown to be of such interest as regards proton structure. The increased y range over which photoproduction can be studied also allows the extraction of the energy dependence of various total and differential cross-sections, such as $\sigma(\gamma p \rightarrow X)$, $\sigma(\gamma p \rightarrow J/\Psi p)$, $\sigma(\gamma p \rightarrow J/\Psi X)$ and $\sigma(\gamma p \rightarrow \rho p)$. Studies of proton structure will also benefit from the proposed upgrade, as one of the remaining uncertainties in these measurements[3, 4] is the contribution made to the proton structure data by high y photoproduction background in which one of the hadrons is mistakenly identified as the scattered electron in the main H1 calorimeters. Clearly identified photoproduction data in the relevant region will allow this background to be quantified more accurately than is currently possible.

2 Detector design

2.1 Introduction

In order to extend the measurable y range up to $y \simeq 0.95$, it is essential that the ET8 be able to detect and measure accurately the energy of electrons with energies as low as 1.5 GeV. Very

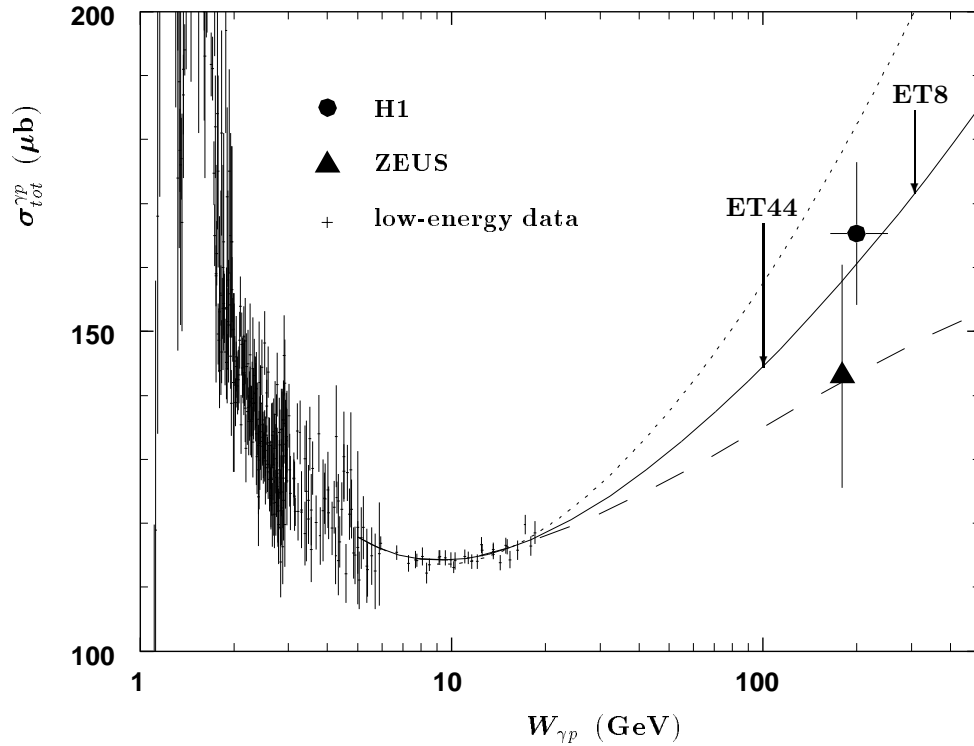


Figure 1: Total photoproduction cross section as a function of the γp centre-of-mass energy $W_{\gamma p}$. The arrows show the energies at which measurements made using the ET44 and the proposed ET8 contribute (820 GeV proton beam).

little space is available in the region in which these electrons leave the beam pipe. The location of the HERA magnets dictates that the ET8 be placed at $z \approx -8$ m, hence its name, and that it be extremely compact. In addition, losses from the proton beam cause large numbers of hadronic interactions in this region, so the ET8 must be radiation hard. To facilitate the separation of the signals due to electrons from those due to hadrons, its response to both must be well understood.

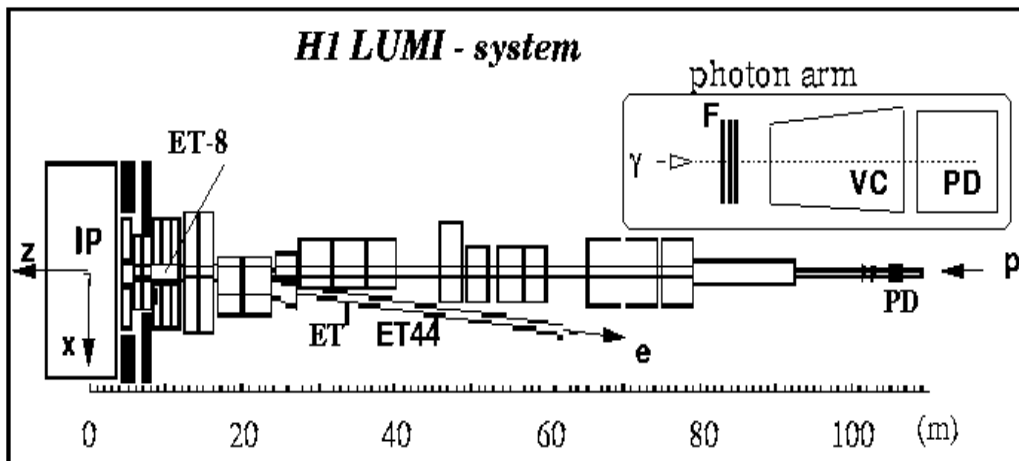


Figure 2: Schematic top view of the H1 luminosity system.

The ET8 is part of the H1 luminosity system, shown in figure 2 and described briefly in the following. A more detailed description of the H1 detector and the luminosity system is given in reference [5].

The luminosity is determined by measuring the rate of photons produced in the Bethe-Heitler process, $ep \rightarrow e\gamma p$. Cross-checks are performed using measurements of the $e\text{-}\gamma$ coincidence rate, the photons and electrons being detected in the calorimeters of the luminosity system. Under normal operating conditions the axis of the photon beam coincides with the axis of the incident electron beam and with the z axis of H1. The bremsstrahlung photons travel inside the proton beam pipe, leave it through an exit window at $z = -92\text{ m}$ and hit the photon arm of the luminosity system, the main part of which is the photon detector (PD) located at $z = -100\text{ m}$. A lead filter (F) and a water Čerenkov veto counter (VC) are located in front of the PD. The filter, of $2X_0$ thickness, absorbs any synchrotron radiation and protects the photon detector against radiation damage. At nominal luminosity the absorbed direct synchrotron radiation power is about 0.4 kW . The VC serves as an additional radiation shield of depth $1X_0$, allows rejection of events in which a photon has converted between the exit window and the photon detector and provides a measurement of some of the energy absorbed before the PD. The scattered electrons are detected in the electron taggers ET and ET44, located at $z = -33.4\text{ m}$ and $z = -44\text{ m}$, respectively. These are total absorption Čerenkov calorimeters made of KRS-15 crystals.

Possible choices for the ET8 included a crystal calorimeter similar to the ET and ET44, a lead-scintillator sampling calorimeter and a spaghetti type calorimeter. For the reasons discussed in the following a spaghetti calorimeter is used, as developed by H1 at DESY for the H1 SpaCal calorimeter [6].

2.2 The new electron tagger

The proposed spaghetti calorimeter consists of BICRON BCF-12 fibres of 0.5 mm diameter embedded in lead, with a lead to fibre ratio of $2.3 : 1$. The resulting Moliere radius is 25.5 mm . The fibres emit blue light with an emission peak near 430 nm . The active volume of the calorimeter is 85 mm deep, corresponding to 10 radiation lengths. The calorimeter has an energy resolution that is about 1.5 times better than that of the ET and ET44 crystal calorimeters. The necessary horizontal spatial resolution is provided by a scintillator hodoscope placed in front of the calorimeter which allows measurement of the horizontal co-ordinate with an accuracy of 1 mm (the width of the scintillator plates is 2 mm). The vertical co-ordinate is determined from the ratio of energy deposited in the upper and lower calorimeter modules. For the majority of events, the electron entry point is near the boundary between these modules, so the accuracy of the vertical co-ordinate determination is better than 1 mm . This spatial resolution ensures that the energy measurement error introduced by corrections for leakage is less than about 5%.

The ET8 is shown in figure 3. A prototype has been built according to this design and tested as discussed later in this paper. Unlike the other calorimeters in the luminosity system, the limited amount of space available demands that the ET8 be installed on a fixed support and stay permanently in the HERA median plane. The two scintillator veto plates placed before and after the scintillator fibres allow rejection of spurious signals due to the passage of particles through the fibres where they exit from the lead and are bundled to enable readout. The intensity of Čerenkov light from particles passing through the light guides is orders of magnitude smaller than the signal from electromagnetic showers in the calorimeter (due partly to the small lateral size of the light guide) so no additional veto is necessary for these.

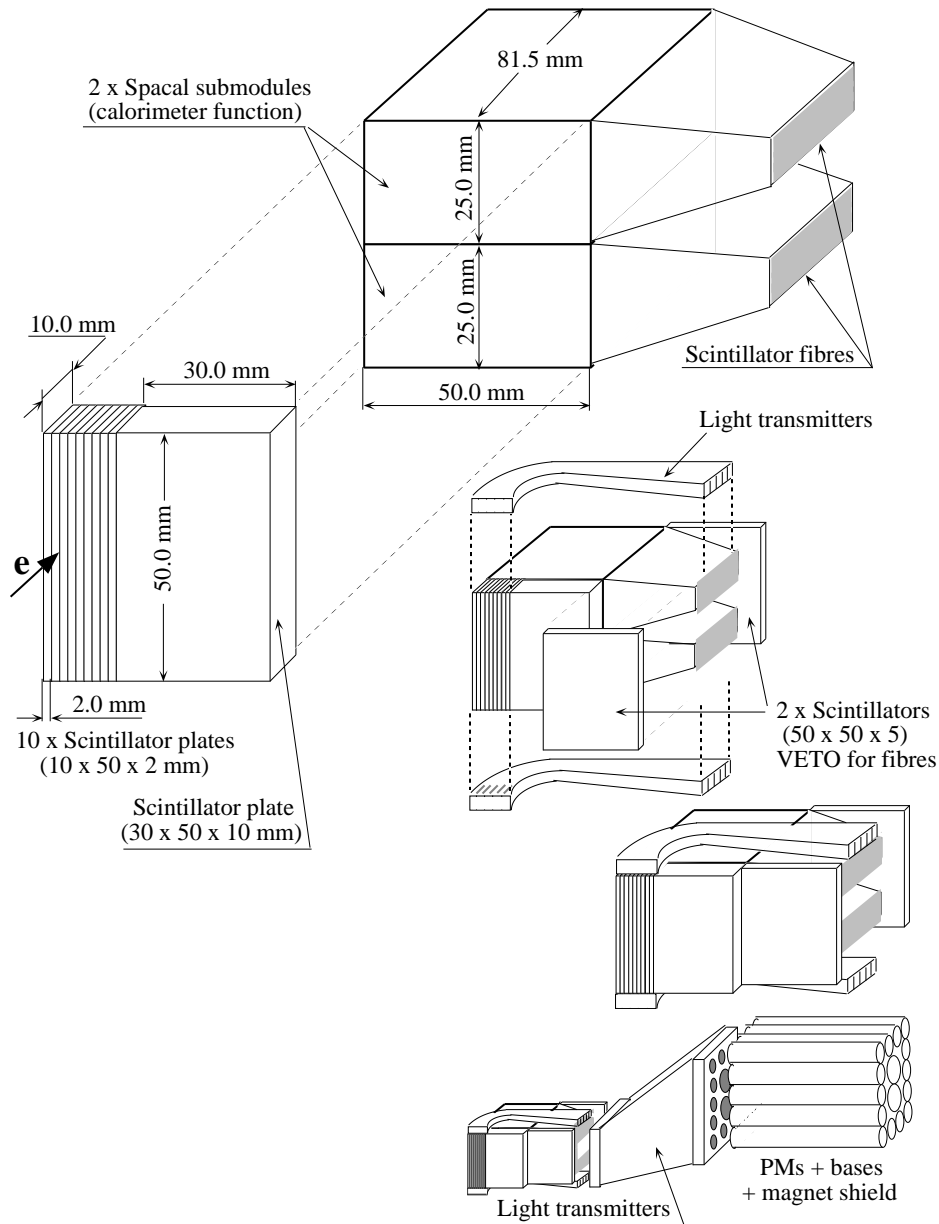


Figure 3: Design of the ET8 calorimeter.

2.3 Acceptance

Acceptance studies have been performed using a fast simulation package, H1LUMI [8]. This models the current HERA electron ring optics as described, for example, in [9]. Several possible positions for the new tagger were considered. After taking into account the apparatus currently present in the HERA tunnel, the space needed for the calorimeter itself and the access requirements for installation and surveying, the position at $z \simeq -8\text{m}$ was chosen. Small possible

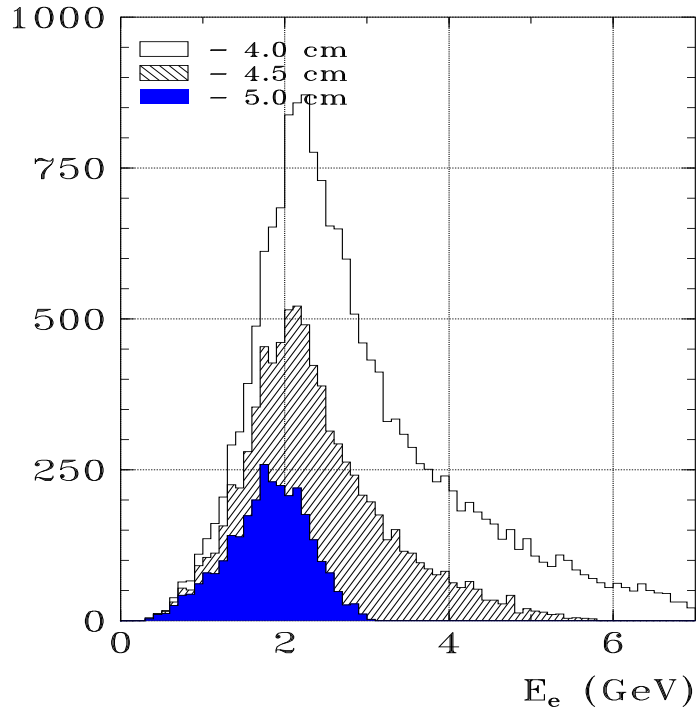


Figure 4: Energy distribution of the scattered electrons in ET8 as a function of distance from the e -beam axis.

variations of the beam parameters at the IP (horizontal and vertical tilt of ± 0.15 mrad and offset of ± 1 mm) were taken into account in the simulation. They typically lead to 15 to 25% changes in the electron tagger acceptance. Variations of ± 1 mm in the detector position give

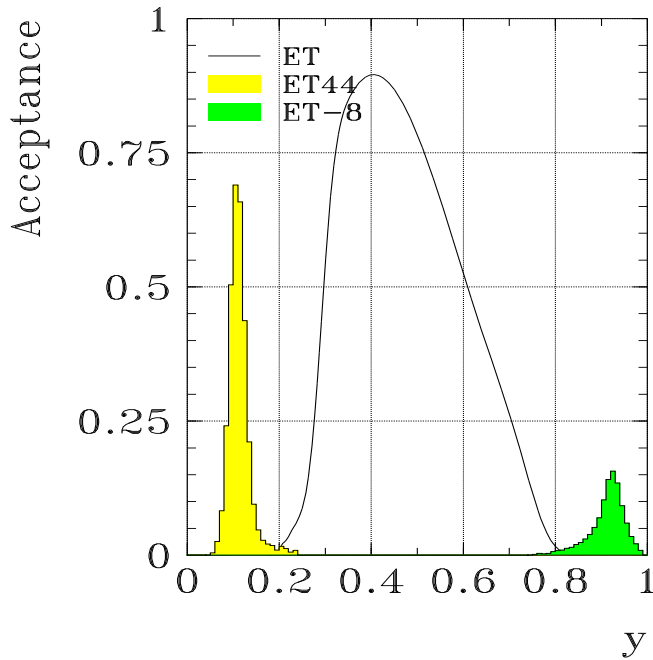


Figure 5: The acceptance for photoproduction events of the three electron taggers with nominal beam conditions.

an uncertainty of about 15% in the ET8 acceptance. Hence, precise knowledge of the both the tagger position with respect to the electron beam and of the beam parameters is very impor-

tant. The acceptance can be defined with high precision from the data using $ep \rightarrow e\gamma p$ events, as is done for the present ET and ET44 calorimeters. This reduces uncertainties related to the precision with which real beam conditions can be simulated. The energy distribution of the

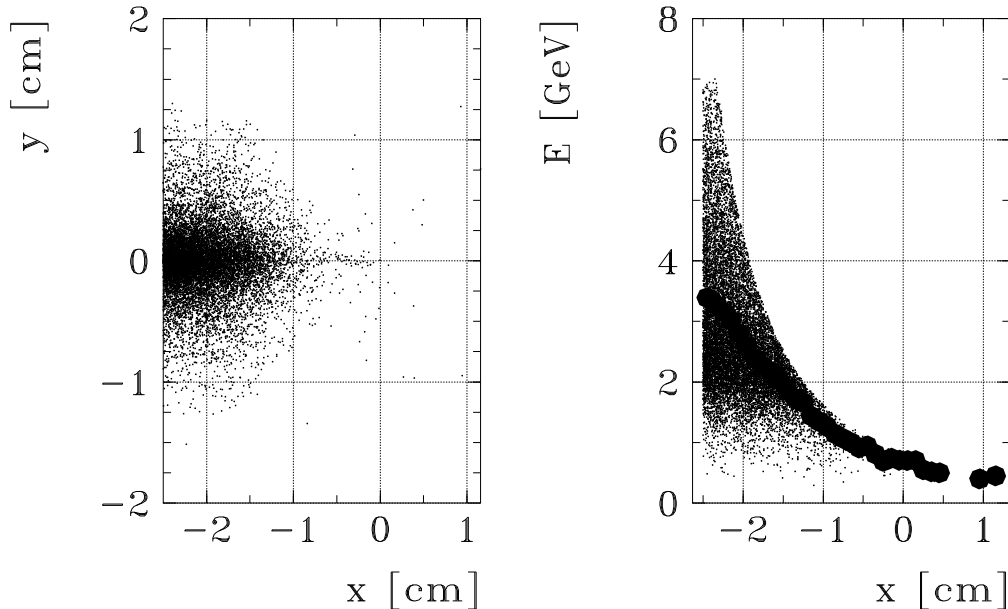


Figure 6: Distribution of co-ordinates of point at which electron enters ET8 (left) and correlation between horizontal co-ordinate of entry point and energy (right) in γp events. Filled circles represent average values with one sigma error bars. The x co-ordinate is measured from the centre of the ET8.

electrons accepted by the ET8 as a function of distance from the electron beam axis is shown in figure 4. Figure 5 shows the acceptances of all the luminosity system electron detectors (ET, ET44 and ET8) for photoproduction events with nominal beam conditions (zero tilt and offset). The ET8 is seen to provide the desired extension of the measurable y range to the high y interval $0.85 < y < 0.95$.

The distribution of the horizontal co-ordinate of the point at which the electron enters the ET8 is shown in figure 6. The lateral size of the calorimeter adequately covers this range. In addition, figure 6 shows the correlation between the measured electron energy and the point at which it enters the detector. This illustrates how precise co-ordinate measurement can aid calibration of the ET8 and reconstruction of the electron energy, in addition to allowing accurate corrections for shower leakage.

2.4 Radiation hardness of materials

The H1 luminosity system, which is close to the HERA beam lines, suffers a considerable radiation load. For example, the PD typically receives a dose of ≈ 10 Mrad during a year's HERA running. Therefore the study of the radiation hardness of the materials (veto scintillators, fibres, plexiglass) used in the ET8 calorimeter is an important task. The influence of radiation on the materials used was studied using the bremsstrahlung photon beam at the 1 GeV electron synchrotron of the Lebedev Physical Institute in Moscow. Samples of the materials to be studied were placed at the beam collimator of the bremsstrahlung beam which is derived from the collision of the accelerated electrons with an internal target. Dose determinations were made using

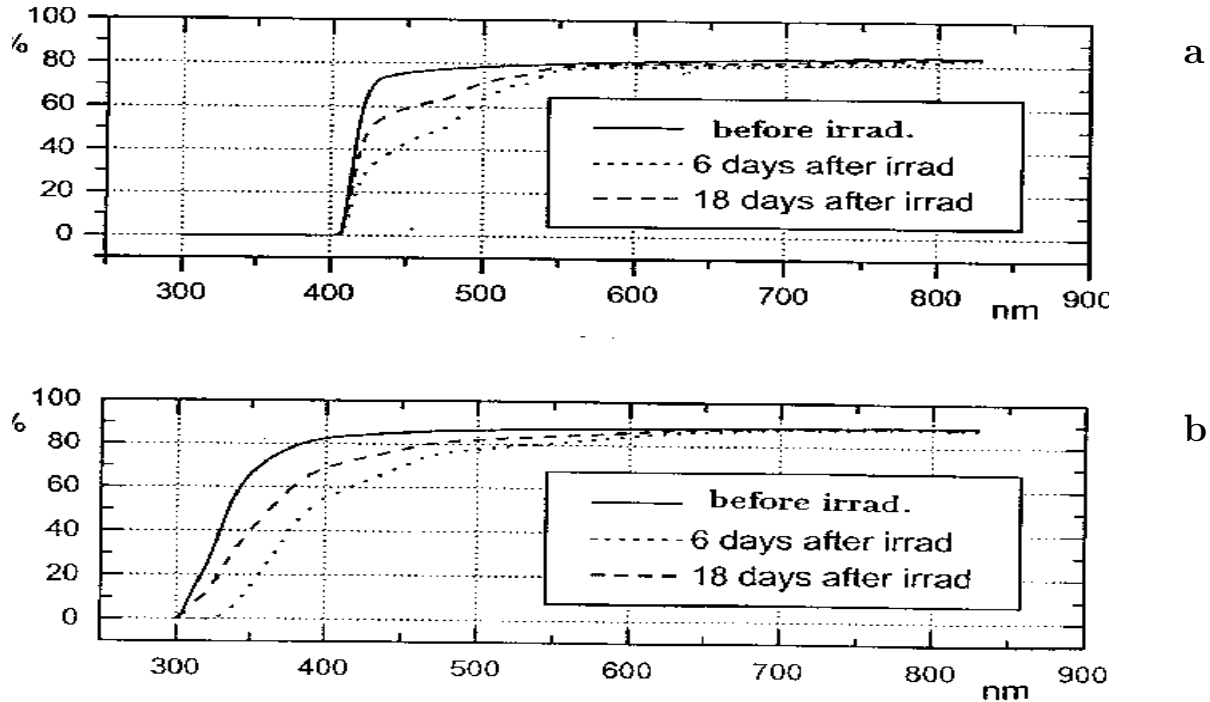


Figure 7: Scintillator (a) and plexiglass (b) optical transmission as a function of wave length λ .

dosimeters adjacent to the samples. Measurements of the change of the attenuation length of the BICRON fibres were made using the procedure described in [7]. The total dose administered to the fibres was 1 Mrad. The measurements show that the photon mean free path decreased from about 130 cm to about 60 cm after irradiation. As the expected yearly dose at the position of the ET8 due to nominal luminosity HERA running is about 0.1 Mrad, the functioning of the calorimeter will not be seriously impaired by the radiation absorbed by the fibres.

The veto scintillator and the plexiglass used as light guides in the ET8 received a total dose of about 2 Mrad. This caused visible yellowing of the scintillator, whereas the plexiglas became brown. The transparency of the samples before and after irradiation in the wavelength range 300 to 800 nm was determined using a spectrophotometer. The results are shown in figure 7. The changes due to the irradiation are seen to be essentially in the short wavelength region. Several days after irradiation the optical transparency was observed to be partially restored.

In conclusion, the tests show that the decrease of the light yield due to the radiation damage suffered by the components of the ET8 will not influence the detector response significantly. The ET8 will be continuously calibrated, as are all the luminosity system detectors. This procedure will correct for the small losses expected under normal HERA operating conditions.

3 Prototype test results

3.1 Design of prototype

A prototype ET8 calorimeter was built according to the design shown in figure 3. In order to test the prototype “in situ”, it was installed in the tunnel as close to the proposed position of the ET8 as was possible. The beam line configuration in 1996 and 1997 required that the prototype ET8 be placed at $z = -7$ m, hence it was dubbed the ET7. Note also that the 1996 and 1997 running was done with positron rather than electron beams.

The level 1 trigger element for the ET7 was the simple condition $E_{tot} > E_{thr}$, where E_{tot} is the sum of the energy deposited in all the calorimeter modules and E_{thr} the threshold energy, which must have a value as low as $E_{thr} \simeq 0.5 \dots 1.0$ GeV. Note that a minimum ionising particle loses about 50 MeV of energy in traversing the ET7. An additional γ -veto condition from the photon arm of the luminosity system suppressed the high rate background from the Bethe-Heitler process with an efficiency of about 98%.

3.2 Event selection and rate

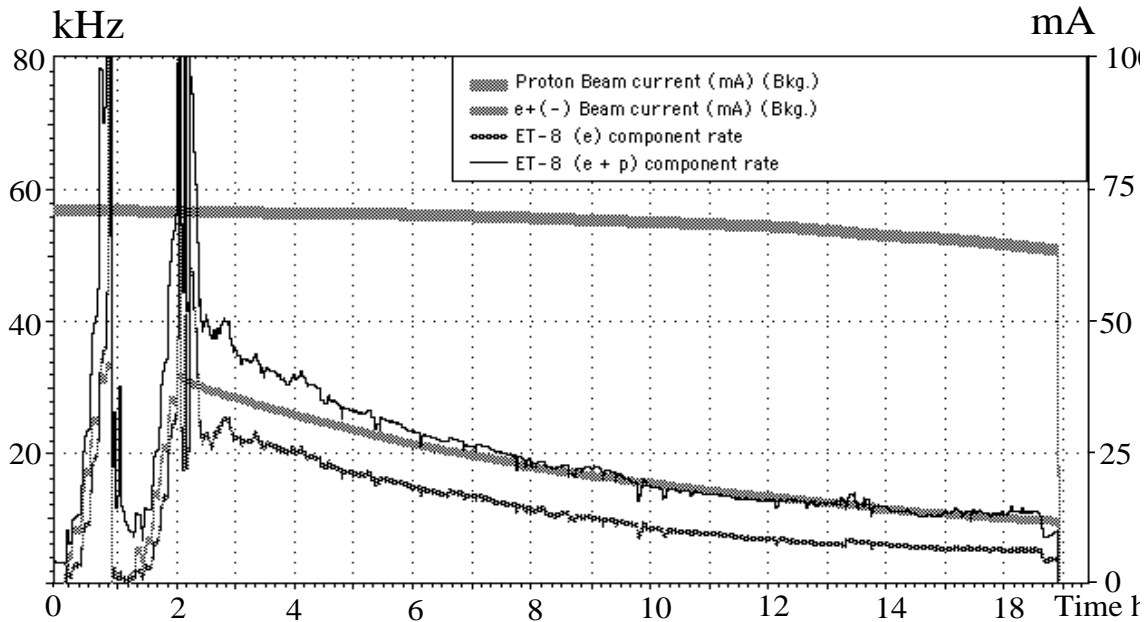


Figure 8: Positron and proton beam currents as a function of time during a luminosity run with the measured rates of ET7 calorimeter triggers with (e) and without ($e + p$) the requirement that the signal be temporally associated with the electron signal. (Note, ET7 labelled ET-8 in figure)

The rate of events observed by the ET7 during one luminosity run is presented in figure 8. The rate spectrum shows spikes caused by particle losses during the injection of the proton and positron beams. Apart from these, the rates are seen to be roughly proportional to the product of the positron and proton beam currents, suggesting that the observed events are predominantly due to positron-proton collisions.

The time structure of the ET7 signals was measured using flash analogue to digital converters. The averaged FADC pulse shape of the calorimeter's response for the events triggered by the ET7 subtrigger is shown in figure 9. Two peaks are seen at different times. The earlier of these is due to the collisions of particles from the proton beam halo with the ET7 and the later to scattered positrons, the time between the two being 54 nsecs as expected given the distance between the interaction point and the ET7. This time difference can be used to isolate the positron signal by defining a "positron time window" about the expected positron time of arrival. This was used to refine the ET7 level one trigger. For the studies described in the following it was required that $E_{thr} = 0.3$ GeV and that the signal from the ET7 be in the positron time window.

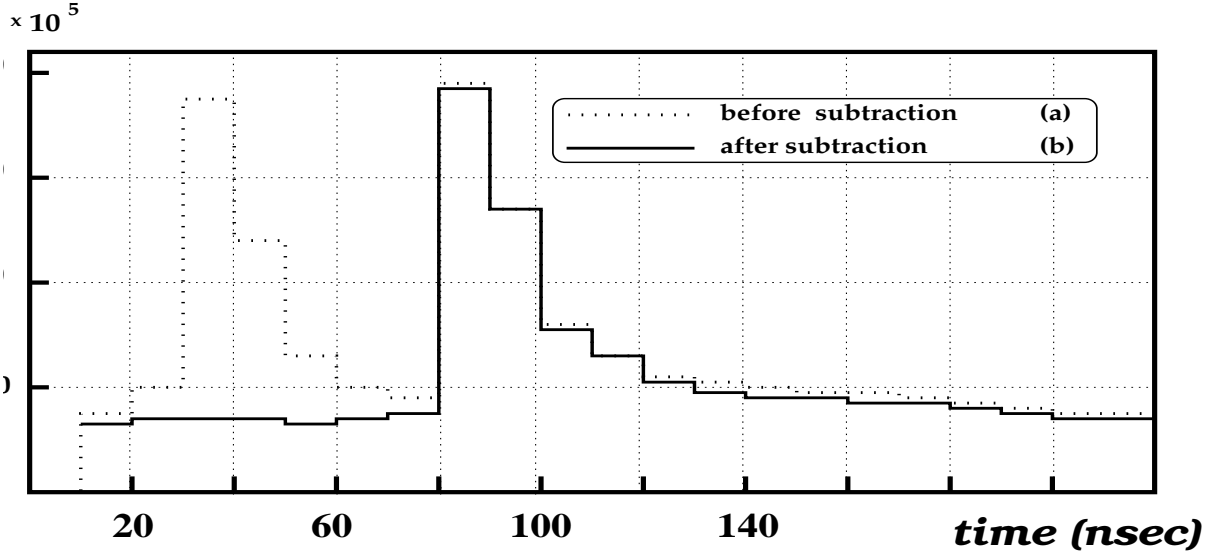


Figure 9: The averaged FADC pulse shape for the events triggered by the prototype ET7 subtrigger (a) with proton halo and (b) after subtraction of proton halo.

3.3 Detector calibration

In common with the other detectors in the luminosity system, $ep \rightarrow e\gamma p$ events are used for energy calibration purposes. Since the energy transfer to the proton is negligible, the relation

$$E'_e + E_\gamma = E_e$$

must hold. The absolute energy scale of the PD can be determined using the high energy edge of the bremsstrahlung spectrum after which the energy detected in the PD, E_{PD} , provides an estimate of E_γ . Studies of the summed energy in the photon arm of the luminosity system and the relevant electron tagger then allow calibration of the latter [10].

The calibration of the ET7 proceeds by selecting events which have a positron impact point on the calorimeter's front plane well removed from its edges. The calibration constants, $C(n)$, of the N ET7 channels are then determined by minimising the expression

$$\sum_i \left(\sum_{n=1}^N C(n) A_i(n) + E_{PD} - E_e \right)^2,$$

where $A_i(n)$ is the amplitude of the signal from the n^{th} channel in the i^{th} event. Using this calibration gives the absolute energy spectrum, measured in the positron time window, shown in figure 10a. The distribution displays the expected peak between 1 and 2 GeV, corresponding to events with $E_\gamma \approx 26$ GeV, that is, $y \approx 0.9$. There is another large contribution to the distribution which is strongly peaked at smaller energies. This is mainly due to background arising from off-momentum positrons accompanying the beam. This can be suppressed by demanding the coincidence of the ET7 signal with a signal from the PD as this selects events from the $ep \rightarrow ep\gamma$ process. The energy distribution of positrons following this selection is presented in figure 10b. There still remains a significant tail to low energy. This is due to the small angle at which the detected positrons traversed the beam-pipe. They travelled through a significant amount of material, often initiating electromagnetic showers and hence depositing only a fraction of their energy in the ET7. This has now been remedied by the installation of a modified beam-pipe with the necessary thin exit window.

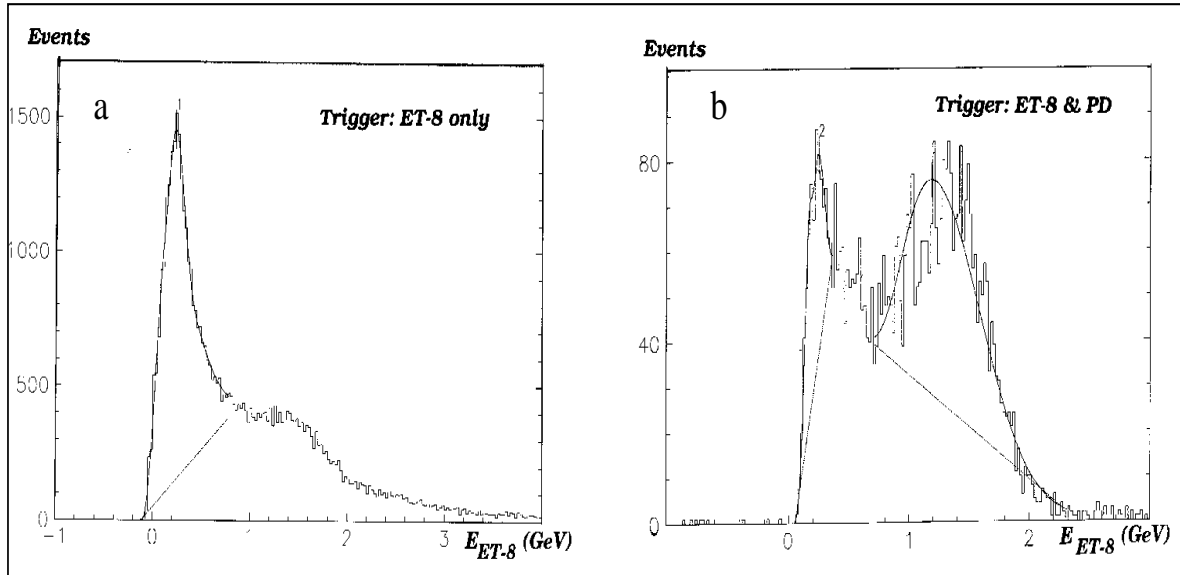


Figure 10: Absolute energy distribution from the prototype ET7 after (a) level one trigger, (b) demanding coincidence with a signal from the photon detector. (Note, ET7 labelled ET-8 in figure.)

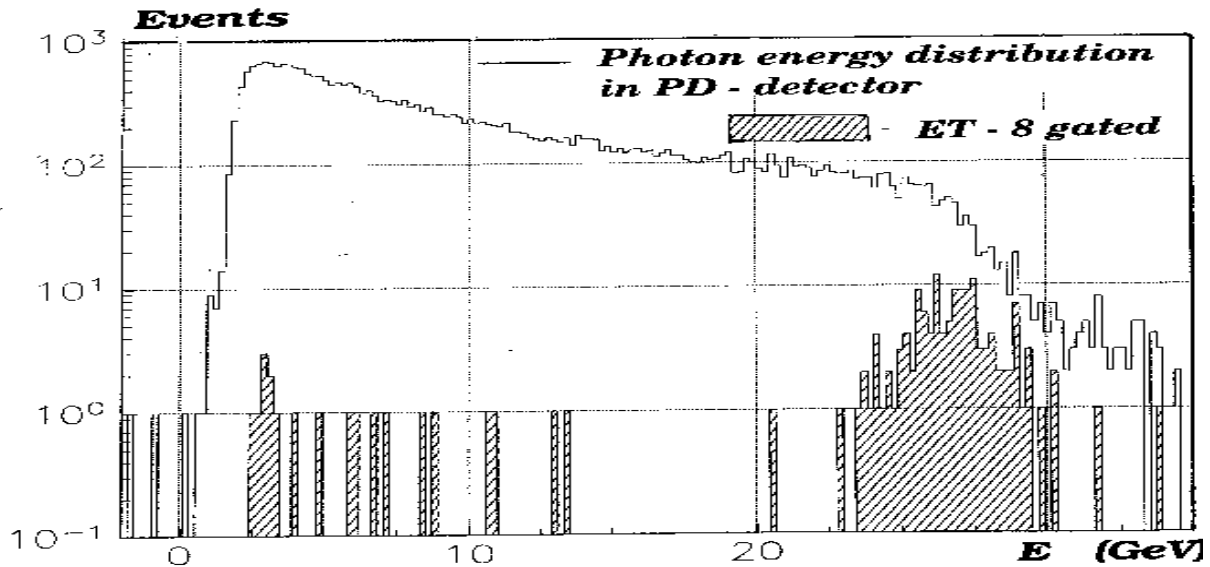


Figure 11: Photon energy spectra measured by the PD: solid line, all measured events; shaded area, events triggered by ET7. (Note, ET7 labelled ET-8 in figure.)

Figure 11 shows the measured energy spectrum of all Bethe-Heitler photons seen in the PD. The shaded area represents events in which the positron was detected in the ET7. Note that the showering in the beam-pipe which occurs in front of the ET7 does not affect this spectrum, and the signal is indeed observed to be very clean. The mean value of this distribution is about 26.2 GeV, which compares well with the expected average energy of bremsstrahlung photons obtained from MC simulations including the effects of the acceptance of the ET7.

Figure 12 illustrates the energy correlation between E_γ and E_{tag} for Bethe-Heitler events

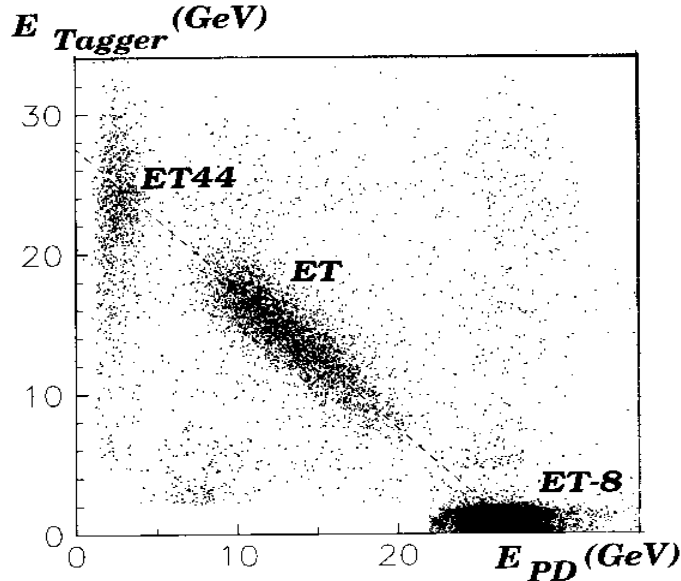


Figure 12: E_γ against E_e for bremsstrahlung events detected by the H1 luminosity system including electron taggers ET, ET44 and ET7. (Note, ET7 labelled ET-8 in figure.)

selected by requiring the coincidence of signals from any one of the ET, the ET44 or the ET7 and the PD. Due to the large differences in the trigger rates of the different taggers, (ET44 \simeq 280 kHz, ET \simeq 170 kHz and ET7 \simeq 15 kHz at a luminosity $\mathcal{L} = 5 \times 10^{30} \text{ cm}^{-2}\text{s}^{-1}$) these data were taken with differing pre-scale conditions for the trigger elements involving the different electron taggers. The anti-correlation arising from the requirement that $E_\gamma + E'_e = E_e$ can clearly be seen. The above demonstrate that the ET7 was indeed detecting and measuring the energy of positrons scattered in $ep \rightarrow ep\gamma$ interactions.

The correlations between the rates of the different taggers within one positron beam filling are presented in figure 13. The measured rates in the taggers are in good agreement with Monte Carlo simulations of bremsstrahlung events including the acceptances of the various taggers.

4 Conclusions

The addition of a new electromagnetic calorimeter, the ET8, to the H1 detector will allow efficient triggering on and measurement of high y photoproduction events. A prototype detector, based on a spaghetti type calorimeter and placed 7 m downstream from the H1 interaction point in the electron direction ($z \approx -7$ m), functioned as expected; adequate energy and position resolution were obtained and the trigger performed well. Following the installation of a modified section of beam-pipe around $z \approx -8$ m, the ET8 has been installed and will allow the study of photoproduction at the highest energies yet achieved during the HERA 1998 and 1999 running.

5 Acknowledgements

We gratefully acknowledge the support of the DESY directorate and the directorate and machine group of the LPI synchrotron (Moscow). We also wish to thank the DESY directorate for the kind hospitality extended to us. We are grateful to P. Biddulph and R. Eichler for their active support and helpful discussions. We would like to thank INTAS, RFBR and the UK PPARC for financial support.

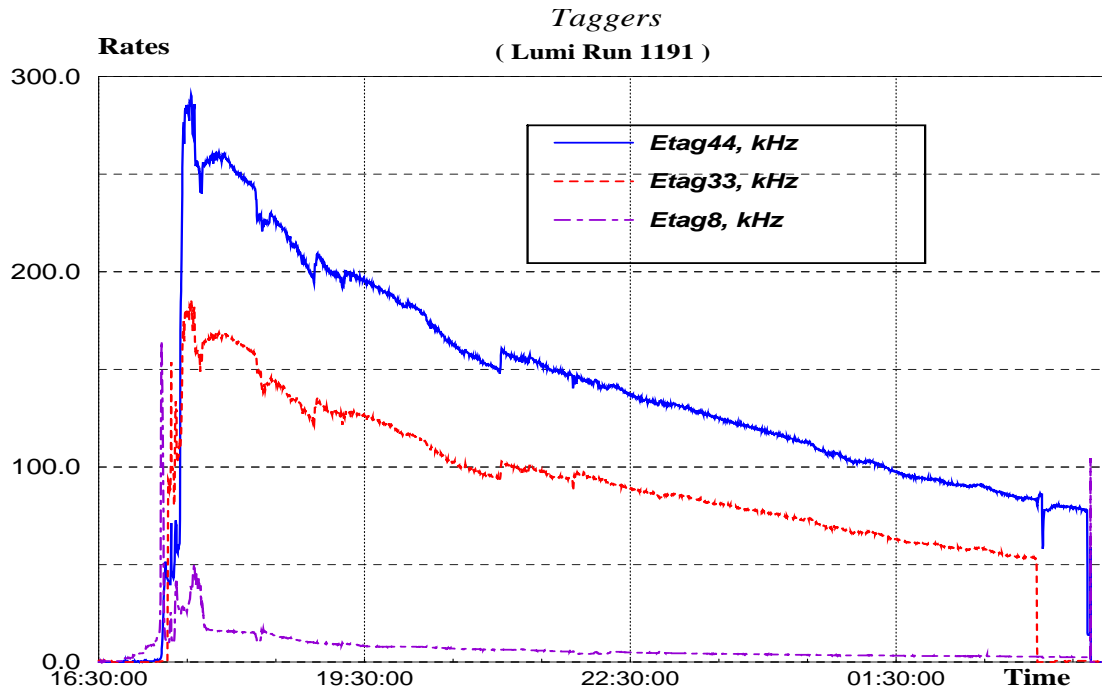


Figure 13: The behaviour of the rates measured in the electron taggers within one beam fill. (Note, ET7 labelled ET-8 in figure.)

References

- [1] S. Aid et al. (H1 Collaboration), *Zeit. Phys.* **C69** (1995) 27.
- [2] C. Adloff et al. (H1 Collaboration), *Eur. Phys. Jour.* **C1** (1998) 97.
- [3] S. Aid et al. (H1 Collaboration), *Nucl. Phys.* **B470** (1996) 3.
- [4] C. Adloff et al. (H1 Collaboration), *Nucl. Phys.* **B497** (1997) 3.
- [5] I. Abt et al. (H1 Collaboration), *Nucl. Inst. Meth.* **A386** (1997) 310; *ibid.* 348.
- [6] T. Nicholls et al. (H1 SpaCal group), *Nucl. Inst. Meth.* **A374** (1996) 149.
- [7] P.S. Baranov, A.S. Belousov, A.I. Lebedev and E.I. Malinovski, "Radiation Hardness of the Scintillating Fibers for the Forward Proton Spectrometer", Intas report, INTAS-93-0043.
- [8] S. Levonian, "H1LUMI - A Fast Simulation Package for the H1 Luminosity System", unpublished H1 note, H1-04/93-287 (1993).
- [9] "HERA Lattice and Optics Design", DESY preprint, DESY HERA 92-07 (1992) 26.
- [10] T. Ahmed et al. (H1 Collaboration), *Zeit. Phys.* **C66** (1995) 529.